(Fig. 2D). Finally, to confirm whether BC-like structures were generated, we added fluorescein diacetate (FDA) to the culture medium after augmenting formation of BC-like structures in the presence of taurocholate (Fu et al., 2011). We found that metabolized fluorescein was excreted into BC-like structures (Fig. 2E). These data indicate that cholangiocytes possessed the ability to convert into functional hepatocytes during the neonatal period.

HNF4α and C/EBPα are induced in neonatal cholangiocytes during culture

Transcription factors have been shown to determine and convert the lineages of many types of cells. At the time when hepatoblasts are committed to cholangiocytes, transcription factors related to hepatocytic differentiation, including HNF4α and CCAAT/enhancer binding protein α (C/EBPα), are suppressed, whereas those related to cholangiocytic differentiation are upregulated (Tanimizu and Miyajima, 2004; Yamasaki et al., 2006). Therefore, we tested the possibility that the expression patterns of these transcription factors differ between neonatal and mature cholangiocytes. We focused on HNF4α and C/EBPα, because both of these are crucial for the differentiation and/or maturation of hepatocytes (Parviz et al., 2003; Mackey and Darlington, 2004). Using quantitative PCR, we examined the expression of *HNF4α* and *C/EBPα* in neonatal and mature cholangiocytes during culture for hepatocytic differentiation. We also examined the expression of *FoxA1* (*HNF3α*), which has been shown to be a crucial factor conferring hepatocytic characteristics on multipotent as well as somatic cells (Sekiya et al., 2009; Sekiya and Suzuki, 2011). HNF4α and C/EBPα genes were clearly induced in neonatal but not in mature cholangiocytes, whereas *FoxA1* was expressed in both cell types (Fig. 3A). These results suggest that the efficient induction of HNF4α and C/EBPα is necessary for cholangiocytes to convert into hepatocytes. Immunofluorescence analysis further confirmed that HNF4α and C/EBPα were induced in neonatal cholangiocytes but not in adult ones after inducing hepatocytic differentiation (Fig. 3B).

Overexpression of C/EBPα and inhibition of the Notch signaling pathway slightly increase hepatocyte gene expression in mature cholangiocytes

To examine whether HNF4α and C/EBPα could induce hepatocytic characteristics, we introduced their cDNAs into mature cholangiocytes using retroviral vectors. Cholangiocytes induced with HNF4α or C/EBPα were sequentially treated with OSM and MG. Both HNF4α and C/EBPα slightly increased expression of albumin, whereas only C/EBPα upregulated *CPSI* (Fig. 3C).

Because the Notch signaling pathway has been implicated in cholangiocyte differentiation of hepatoblasts and hepatocytes (Tanimizu and Miyajima, 2004; Zong et al., 2009), we considered a possibility that constitutive activation of the pathway might inhibit hepatocytic differentiation of adult cholangiocytes. Therefore, we also examined whether inhibition of the Notch pathway by adding 3,5-difluorophenylacetyl-L-alanyl-L-2-phenylglycine *t*-butyl ester (DAPT), a γ-secretase inhibitor that potentially blocks the Notch signaling pathway (Sastre et al., 2001), could induce the hepatocytic differentiation of mature cholangiocytes. The DAPT treatment slightly decreased expression of *Hes1*, one of major targets of the

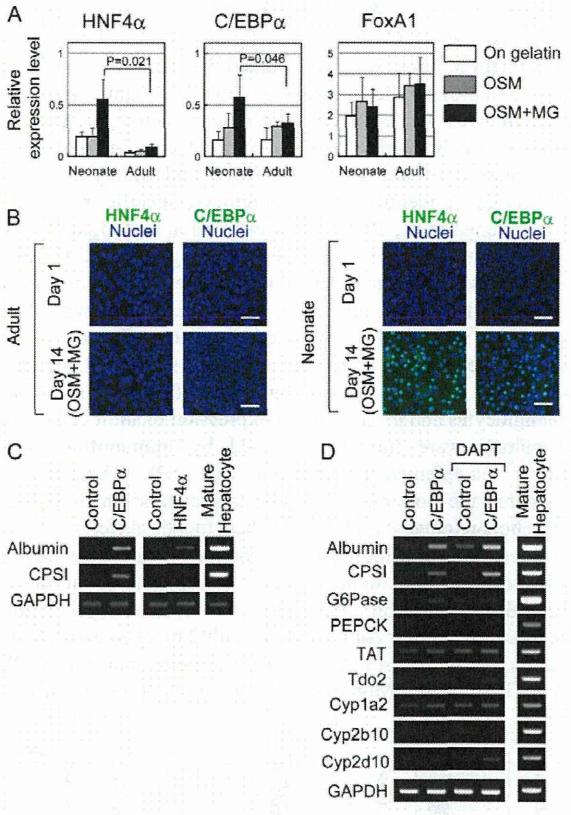

Fig. 3. Overexpression of C/EBPα slightly induces CPSI expression in adult cholangiocytes. (A) Expression of HNF4α, C/EBPα and FoxA1 in cholangiocytes during culture. HNF4α and C/EBPα were induced in neonatal cholangiocytes but not in adult cholangiocytes. FoxA1 was expressed in both types of cells. Expression levels are presented relative to the expression levels in MHs cultured for 1 day. Two-tailed Student's *t*-tests were performed using Microsoft Excel. (B) Protein expression of HNF4α and CPSI. HNF4α and C/EBPα proteins were induced in neonatal cholangiocytes after inducing hepatocytic differentiation. Nuclei were counterstained with Hoechst 33258. Scale bars: 50 μm. (C) Expression of CPSI was induced by the overexpression of C/EBPα, but not HNF4α. (D) Induction of hepatocyte markers by overexpression of C/EBPα in the presence of a γ-secretase inhibitor. Expression of albumin and CPSI hepatocytic induced by C/EBPα was further upregulated in the presence of DAPT, a γ-secretase inhibitor and a potent inhibitor for the Notch signaling pathway. The data also show that expression of Tdo2 and Cyp2d10 were slightly increased.

Notch pathway, whereas expression of albumin was significantly increased in the presence of DAPT (supplementary material Fig. S6).

Next, we examined whether overexpression of C/EBPα and inhibition of the Notch pathway have an additive effect on hepatocytic differentiation. As shown in Fig. 3D, albumin and *CPSI* were induced to a greater extent by a combination of DAPT and C/EBPα expression than by the treatment of either of them alone. *Tdo2* and *Cyp2d10* were slightly induced by the combination of DAPT with C/EBPα. Although the level of expression of hepatocyte markers was much lower than in MHs, C/EBPα expression affected the differentiation status of mature cholangiocytes.

Grainyhead-like 2 inhibits hepatocytic differentiation

Overexpression of C/EBPα only slightly promoted hepatocytic differentiation. Therefore, we assumed that molecular machinery strongly stabilizing the cholangiocyte lineage might exist in adult cholangiocytes. As candidates of inhibitory factors, we examined expression of cholangiocytic transcription factors including Sox9, hairy-enhance of slit 1 (Hes1), Hey1 and grainyhead-like 2 (Grhl2) that we identified as cholangiocyte-specific transcription factors (Senga et al., 2012). Their expression was higher in adult cholangiocytes than in neonatal cells (Fig. 4A). Furthermore, Grhl2 and Hes1 were maintained at lower levels in neonatal cells than in adult cells during culture (Fig. 4B). Interestingly, Grhl2 expression was further inhibited in neonatal culture after inducing hepatocytic differentiation by sequential treatment with OSM and MG. Downregulation of Grhl2 in neonatal cholangiocytes and its continuous expression in adult cells during the culture were further confirmed by immunofluorescence analysis (supplementary material Fig. S7). Therefore, we considered the possibility that constant expression of Grhl2 in adult cholangiocytes might inhibit hepatocytic differentiation.

To test this hypothesis, we introduced Grhl2 into neonatal cholangiocytes and induced hepatocytic differentiation, and found that Grhl2 inhibited induction of hepatocyte markers (Fig. 4C). We further confirmed that Grhl2 blocked expression of albumin, CPSI, HNF4α, and C/EBPα proteins induced by OSM and MG (Fig. 4D). Moreover, the downregulation of Grhl2 by short interfering RNAs (siRNAs) in adult cholangiocytes slightly induced hepatocytic characteristics (supplementary material Fig. S8). These results suggest that maintenance of Grhl2 at a high level is a crucial factor fixing adult EpCAM$^+$ cells in the cholangiocyte lineage.

Epithelial characteristics of neonatal and adult cholangiocytes

Given that Grhl2 is implicated in maturation of cholangiocytes (Senga et al., 2012), we considered the possibility that neonatal and adult cholangiocytes might be different in terms of their maturation status as epithelial cells, although bile duct structures are formed in neonatal liver (Fig. 5A). To examine epithelial characteristics of cholangiocytes, we cultured them to develop monolayers, and first measured transepithelial resistance (TER). In the culture condition used here, cholangiocytes formed a monolayer during 2 days of incubation. During and after the formation of the monolayers by neonatal and adult cholangiocytes, values of TER increased and reached a plateau (supplementary material Fig. S9). After 4 days of incubation, the monolayer of adult cholangiocytes showed the higher TER value than that of neonatal cells (Fig. 5B). We also examined the efflux of 4 kDa fluoresceinisothiocyanato-dextran (FITC-dextran) and found that FITC-dextran passed through the monolayer derived from neonatal cholangiocytes more readily than through that of adult cells (Fig. 5C). These results indicated that neonatal

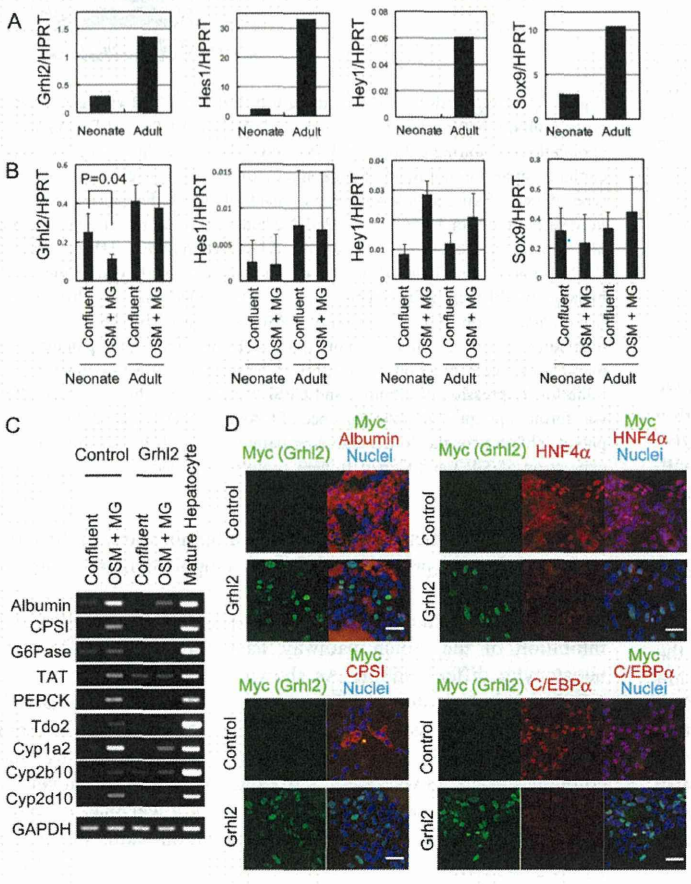

Fig. 4. Overexpression of Grhl2 inhibits hepatocyte conversion of neonatal cholangiocytes. (A) Cholangiocyte transcription factors are expressed more in neonatal cholangiocytes than in adult ones. Neonatal and adult cholangiocytes were isolated from 1W and 8W livers, respectively, as EpCAM$^+$ cells by FACS. Expressions of *Grhl2*, *Hes1*, *Hey1* and *Sox9* were examined by quantitative PCR. Neonatal and adult cholangiocytes were isolated from six and three mice, respectively, as EpCAM$^+$ cells by FACS. Cell isolation was repeated four times, independently. The expression levels are shown relative to that of adult cholangiocytes. (B) The expression of cholangiocyte transcription factors is changed during the culture of cholangiocytes. Expression of Grhl2 was downregulated in neonatal cholangiocytes during hepatocytic differentiation, whereas it was maintained in adult cells during culture. Expression of Hes1 in neonatal cholangiocytes remained at a lower level compared with adult cells. However, in contrast to Grhl2, Hes1 was not further downregulated during hepatocytic differentiation of neonatal cholangiocytes. Culture was repeated three times, independently. Error bars represent s.d. Two-tailed Student's *t*-tests were performed using Microsoft Excel. (C) Grhl2 inhibits hepatocytic differentiation of neonatal cholangiocytes. Grhl2 was introduced to neonatal cholangiocytes. Hepatocytic differentiation was induced by OSM and MG. Grhl2 inhibited the induction of hepatocytes markers. Cultures were repeated three times, independently. (D) Grhl2 inhibits expression of albumin, CPSI, HNF4α and C/EBPα proteins. Neonatal cholangiocytes introduced with the control vector or the vector containing Grhl2 were treated with OSM and MG. Expression of albumin, CPSI, HNF4α and C/EBPα was examined by immunostaining (red). Myc-tagged Grhl2 was detected by anti-Myc antibody (green). Scale bars: 50 μm.

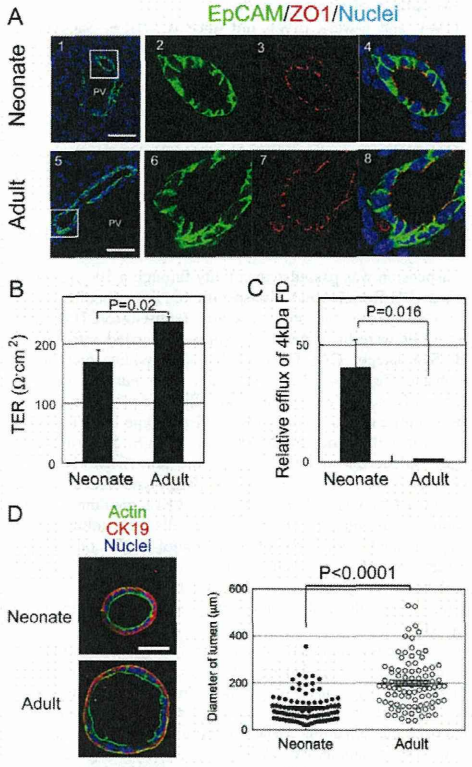

Fig. 5. Neonatal cholangiocytes are immature epithelial cells as compared with adult cells. (A) Bile ducts are present in neonatal and adult livers. EpCAM^{+} cholangiocytes form bile ducts in neonatal (1W-old) and adult livers. Tight junctions, recognized by ZO1 staining, are present around the lumens of neonatal and adult bile ducts. Liver sections were incubated with anti-EpCAM (green) and anti-ZO1 (red) antibodies. Nuclei were counterstained by Hoechst 33258. Boxes in panels 1 and 5 are enlarged in panels 2–4 and 6–8, respectively. Scale bars: 50 μm. (B) Neonatal cholangiocytes have a lower TER value. Fifty thousand cholangiocytes were plated onto Col-I gel in a 12-well plate. TER values at day 4 are shown in the graph. Cultures were repeated three times, independently. Bars indicate s.e.m. Two-tailed Student's *t*-tests were performed. (C) Higher paracellular efflux of 4 kDa FD occurs through the monolayer of neonatal cholangiocytes. At day 4 of culture, paracellular efflux of 4 kDa FITC-dextran (FD) was examined for the monolayers of neonatal and adult cholangiocytes. Bars indicate s.e.m. Two-tailed Student's *t*-tests were performed. (D) Neonatal cholangiocytes form smaller cysts than adult cells in 3D culture. Neonatal and adult cholangiocytes dissociated from Col-I gel were incubated in gel containing 5% Matrigel. Representative neonatal and adult cysts are shown in the left panels. Scale bar: 50 μm. After incubation for 10 days, the diameter of the lumen was measured. Cultures of neonatal and adult cholangiocytes were repeated three and two times, respectively. Each culture was performed in four wells. A dot plot is shown with bars indicating the means ± s.e.m.

cholangiocytes formed relatively immature tight junctions (TJs) compared with adult cells.

As we previously reported, maturation of TJs promotes epithelial morphogenesis, which could be correlated with enlargement of the apical lumen of cysts formed in three-dimensional culture of epithelial cells (Senga et al., 2012). After 10 days of three-dimensional culture, about 1% of neonatal and adult cholangiocytes formed cysts with a central lumen. However, the lumen size of neonatal cysts was significantly ($P<0.0001$) smaller than that of adult cysts, further suggesting that neonatal cells form relatively immature TJs compared with adult ones (Fig. 5D). These results indicate that neonatal cholangiocytes are immature epithelial cells.

Discussion

In this study, we demonstrated that cholangiocytes possess the ability to convert into hepatocytes in the neonatal period but this capability is lost in the adult. Similarly, it has been demonstrated that pancreatic duct cells have the potential to differentiate into endocrine and exocrine cells in the neonatal period but their differentiation potential becomes limited in the adult (Kopp et al., 2011). Thus, tubular epithelial cells may generally lose lineage plasticity during postnatal development.

Although, as we mentioned above, it has been shown that neonatal pancreatic duct cells lose the capability to differentiate to multiple types of cell during development, it is not known how the plasticity of epithelial cells is limited. We unexpectedly found that neonatal cholangiocytes are still developing epithelial characteristics even after forming the tubular structure. It can be assumed that production of bile by neonatal hepatocytes is less than that by mature ones and, therefore, relatively immature TJs in neonatal livers are sufficient to prevent the leakage of bile to the parenchyma and/or to the blood vessels, including the portal vein and the hepatic artery. This assumption seems to be consistent with the fact that the accumulation of bile in the neonatal gallbladder is much less than in the adult one (supplementary material Fig. S10). Furthermore, we showed that Grhl2 was expressed at a higher level in adult than in neonatal cholangiocytes and could inhibit hepatocytic differentiation. As we previously demonstrated, Grhl2 promotes formation of functional TJs by establishing a molecular network among claudin 3, claudin 4 and Rab25 (Senga et al., 2012). Thus, our results suggest that the molecular machinery that establishes the epithelial integrity limits the differentiation potential of epithelial cells and thereby stabilizes the lineage of the cells.

It was recently shown that transcription factors could covert fibroblasts into pluripotent stem cells or other types of somatic cells (Yamanaka and Blau, 2010; Yang, 2011). The combination of Gata4, HNF1α and FoxA1, or that of HNF4α plus FoxA1, A2 or A3, was able to convert mouse skin fibroblasts to hepatocytes (Huang et al., 2011; Sekiya and Suzuki, 2011). Because these proteins are strongly expressed in MHs but not in cholangiocytes, we considered the possibility that their expression status is a key to determining the potential for hepatocytic differentiation. In addition to these transcription factors, we focused on C/EBPα, which is also important for the functions of MHs (Inoue et al., 2004). During the course of hepatocytic differentiation, neonatal cholangiocytes expressed FoxA1, HNF4α and C/EBPα. Adult cholangiocytes, however, expressed FoxA1 but neither HNF4α nor C/EBPα. To elucidate the difference in induction, we examined epigenetic modification of the promoters of HNF4α and C/EBPα. Compared with hepatocytes, methylation of CpG sequences increased in cholangiocytes (supplementary material Fig. S11). However, there was little difference between 1W and 6W cholangiocytes. Other epigenetic mechanisms or upstream factors may regulate the expression of HNF4α and C/EBPα in hepatic epithelial cells. Although C/EBPα expression was effective in conferring hepatocytic characters on cholangiocytes,

the level of induction was limited. This indicates that other factors may block lineage conversion. The present study suggests that Grhl2 is one such inhibitory factor.

Although Grhl2 did not affect expression of C/EBPα mRNA, it did block induction of C/EBPα protein during hepatocytic differentiation (supplementary material Fig. S12; Fig. 4), suggesting that Grhl2 or its target inhibits translation of C/EBPα. However, downregulation of Grhl2 alone did not markedly induce expression of C/EBPα and hepatocytic differentiation in adult cholangiocytes. This result indicates that other molecules might be involved in regulating those processes. Nevertheless, when upregulation of C/EBPα and downregulation of Grhl2 simultaneously occurred in adult cholangiocytes, hepatocytic markers were further upregulated and some cells expressed albumin and CPSI proteins (supplementary material Fig. S13). Moreover, we demonstrated that the inhibition of the Notch pathway by DAPT was effective in inducing hepatocytic characteristics in adult cholangiocytes, although DAPT treatment only slightly upregulated Hes1. Given that the Notch pathway could regulate the lineage of hepatic epithelial cells independently of Hes1 (Jeliazkova et al., 2013), other targets of the pathway may be also involved in conferring hepatocytic characteristics in adult cholangiocytes. Taken together our results suggest that to induce hepatocytic differentiation in adult cholangiocytes, we may need to not only promote expression of hepatocytic transcription factors but also inhibit cholangiocytic factors and the Notch pathway.

In summary, we demonstrate here that cholangiocytes alter their lineage plasticity during epithelial maturation. We identified a possible molecular network augmenting epithelial structures and functions, which also contributes to stabilization of the epithelial cell lineage by blocking conversion to other lineages. Our results suggest that it is not easy to convert the mass of mature cholangiocytes to hepatocytes; however, several groups have reported that hepatocytes can be produced from pluripotent stem cells or somatic cells (Si-Tayeb et al., 2010; Huang et al., 2011; Sekiya and Suzuki, 2011). Although induced hepatocytes differentiate to functional hepatocytes in diseased mice, it is still difficult to control the process of hepatocytic differentiation of pluripotent and somatic cells and produce a mass of MHs *in vitro*. Neonatal cholangiocytes have a remarkably strong ability to convert into hepatocytes, so for pluripotent cells to achieve the differentiation status of these cells would be an important step in the differentiation process. We have successfully expanded human cholangiocytes isolated from adult human liver tissue in the same culture conditions as used for mouse cholangiocytes (supplementary material Fig. S3). In addition, cholangiocytes isolated from extrahepatic bile ducts and the gallbladder of adult mice could proliferate efficiently in the same culture conditions (data not shown). Therefore, if we could find a factor that reverts mature cholangiocytes to the differentiation status of neonatal ones, it may be possible to produce functional hepatocytes that can be used as a source of cell therapy and for drug screening.

Materials and Methods

Extracellular matrix, growth factors and chemicals

Col-I (3 mg/ml) was purchased from Koken Co., Ltd (Tokyo, Japan). Growth factor-reduced Matrigel® (MG), which contains extracellular matrix proteins including type IV collagen, laminin-111 and nidogen, was purchased from BD Biosciences (Bedford, MA). Epidermal growth factor (EGF), hepatocyte growth factor (HGF) and OSM were purchased from R&D Systems (Minneapolis, MN).

Isolation and culture of cholangiocytes

One-week (1W)- and 6-week (6W)- old mice (C57BL6, Sankyo Lab Service, Japan) were used to isolate neonatal and adult cholangiocytes, respectively. All the animal experiments were approved by the Sapporo Medical University Institutional Animal Care and Use Committee and were carried out under the institutional guidelines for ethical animal use. A two-step collagenase perfusion method was performed through the portal vein of adult mice or through the left ventricle of neonatal mice to digest liver tissues. After the removal of parenchymal cells, the residual material including bile ducts was further digested with Liberase TM (Roche Applied Sciences, San Diego, CA) for neonatal tissues or with collagenase/hyaluronidase solution for adult tissues. Enzymatic digestion was terminated by adding ice-cold fresh medium containing 10% fetal bovine serum (FBS).

The cell suspension was passed sequentially through a 100-μm mesh and a 70-μm cell strainer (BD Biosciences). Nonspecific binding of antibodies was blocked by an antibody against the Fcγ receptor (anti-CD16/CD32 antibody; BD Biosciences). Cells were incubated with biotin-conjugated anti-EpCAM antibody (BioLegend, San Diego, CA) followed by streptavidin microbeads (Miltenyi Biotec, Gladbach, Germany). $EpCAM^+$ cells were purified through a MACS column (Miltenyi Biotec). Twenty thousand cells were placed in each well of a 12-well plate. For culture on Col-I gel or MG, collagen type IAC (Koken) mixed with 10× reconstitution buffer containing 200 mM HEPES, 50 mM NaOH, 260 mM $NaHCO_3$, 10× Dulbecco's modified Eagle's medium (DMEM) and PBS or MG was added to each well. To coat wells with collagen type IAC or MG, these agents were diluted in 0.1 M CH_3COOH and DMEM/F12 medium, respectively, and 500 μl of solution was added to each well. The cells were cultured in DMEM/F12 medium supplemented with 10% FBS, 10 ng/ml EGF and HGF, 5×10^{-8} M dexamethasone (Dex; Sigma Chemical Co., St. Louis, MO) and 1× insulin-transferrin-selenium (ITS; Gibco, Carlsbad, CA). After 5–7 days in culture, cells were dissociated from the dishes and then used for subculture (supplementary material Fig. S1).

Human liver tissue was obtained from a patient who underwent hepatic resection at Sapporo Medical University Hospital, with informed consent and the approval of the Sapporo Medical University Ethics Committees. The liver tissue was digested by a method reported previously (Sasaki et al., 2008). Cholangiocytes were isolated from the remaining tissue using the same protocol as that used for the isolation of mouse cholangiocytes and then purified through an MACS column with FITC-conjugated anti-human EpCAM (BioLegend) and anti-FITC microbeads (Miltenyi Biotec).

Induction of hepatocytic differentiation

After culture on Col-I gel, cholangiocytes were dissociated from the gel and 5×10^4 cells were cultured in each well of 24-well plates coated with gelatin. After the cells became confluent, they were incubated with 20 ng/ml OSM, 1% DMSO, 10^{-7} M Dex, and 1× ITS for 4 days and then overlaid with 5% MG for an additional 4 days.

To examine the ability to eliminate ammonium ions from the culture medium, NH_4Cl was added to the culture medium at 2 mM. The concentration of ammonium ions was measured every 2 hours by using the Ammonia Test Wako (Wako Pure Chemical Industries, Osaka, Japan).

To enhance the formation of bile canaliculus (BC) structures in the colonies, 100 μM taurocholate (Tokyo Chemical Industry Co. Ltd, Tokyo, Japan) was added to the medium for 1 day. The formation of BC-like structures was confirmed by incubation with 10 μg/ml fluorescein diacetate (FDA; Sigma-Aldrich, St. Louis, MO) for 30 minutes. The accumulation of metabolized fluorescein into BC-like structures was examined.

Overexpression of transcription factors

cDNAs of C/EBPα, HNF 4α and Grhl2 were amplified by PCR and inserted into retroviral vectors to generate pMXsNeo-C/EBPα, pMXsPuro-HNF4α and pMXsNeo-Grhl2. Retrovirus was added to the culture 48 hours after starting the culture on Col-I gel. For the control, pMXsNeo or pMXsPuro was introduced to cholangiocytes. G418 (1 mg/ml) or puromycin (10 μg/ml) was added to the culture 24 hours after infection to select cells with pMXsNeo-C/EBPα or pMXsNeo-Grhl2, and pMXsPuro-HNF4α, respectively. After incubation in the presence of antibiotics for 24 hours, cells were incubated in medium without them for 2 or 3 days before replating onto gelatin-coated dishes.

PCR

Total RNA was isolated from purified $EpCAM^+$ cells using an RNeasy Mini Kit (Qiagen, Hilden, Germany). cDNA was synthesized using an Omniscript Reverse Transcription Kit (Qiagen). Primers used for PCR are shown in supplementary material Table S1.

Immunofluorescence chemistry

Cholangiocytes induced to differentiate or colonies derived from $EpCAM^+$ cells were fixed in PBS containing 4% paraformaldehyde (PFA) at 4℃ for 15 minutes.

After permeabilization with 0.2% Triton X-100 and blocking with Blockace (DS Pharma, Biomedical Co. Ltd, Osaka, Japan), cells were incubated with primary antibodies (supplementary material Table S2). Signals were visualized with Alexa-Fluor-488, -555 or -633-conjugated secondary antibodies (Molecular Probes, Carlsbad, CA). Nuclei were counterstained with Hoechst 33258. Images were acquired with a Nikon X-81 fluorescence microscope.

Measurement of TER and paracellular tracer flux

Fifty thousand cholangiocytes dissociated from the Col-I gel were replated on a 12 mm Transwell with a 0.4 μm pore, polyester membrane coated with Col-I gel, which was placed in a 12-well plate (Corning Inc., Corning, NY). TER was measured directly in the culture medium using a Millicell-ERS epithelial Volt–Ohm meter (Millipore, Billerica, MA) during the culture. The TER values were calculated by subtracting the background TER of blank filters, followed by multiplying by the surface area of the filter (1.12 cm^2). For the paracellular tracer flux assay, 4 kDa FITC-dextran (Sigma-Aldrich) was added to the medium inside the Transwell dish on day 4 at a concentration of 1 mg/ml. After incubation for 2 hours, an aliquot of medium was collected from the basal compartment. The paracellular tracer flux was determined as the amount of FITC-dextran in the basal medium, which was measured with an Infinite M1000 Pro multi-plate reader (Tecan Group Ltd, Mannedorf, Switzerland).

Three-dimensional culture

Neonatal and adult cholangiocytes were cultured in gel containing Matrigel® as previously reported (Tanimizu et al., 2007). Briefly, cholangiocytes were dissociated from Col-I gel and 5,000 cells were replated on the mixture of Matrigel® and type I collagen (1:1 v/v) in a well of an 8-well coverglass chamber (Nunc, Roskilde, Denmark) covered with 5% Matrigel®. After 5 minutes of incubation, cells were fixed and used for immunofluorescence analysis.

Acknowledgements

We thank Ms Minako Kuwano and Ms Yumiko Tsukamoto for technical assistance.

Author contributions

N.T., study concept and design, acquisition and analysis of data, writing the manuscript, obtained funding; Y.N., sample preparation; N.I., discussion about data, T.M., sample preparation and obtained funding; K.H., obtained funding; T.M., editing the manucscript, obtained funding.

Funding

This work was supported by the Ministry of Education, Culture, Sports, Science and Technology, Japan, Grants-in-Aid for Young Scientists (B) [grant number 22790386 to N.T.]; Innovative Area [grant number 24112519 to N.T.]; and Grants-in-Aid for Scientific Research (B) [grant numbers 22390259 to K.H. and 21390365, 24390304 to T.M.].

Supplementary material available online at
http://jcs.biologists.org/lookup/suppl/doi:10.1242/jcs.133082/-/DC1

References

Espanol-Suner, R., Carpentier, R., Van Hul, N., Legry, V., Achouri, Y., Cordi, S., Jacquemin, P., Lemaigre, F. and Leclercq, I. A. (2012). Liver progenitor cells yield functional hepatocytes in response to chronic liver injury in mice. *Gastroenterology* **143**, 1564-1575, e1567.

Fu, D., Wakabayashi, Y., Lippincott-Schwartz, J. and Arias, I. M. (2011). Bile acid stimulates hepatocyte polarization through a cAMP-Epac-MEK-LKB1-AMPK pathway. *Proc. Natl. Acad. Sci. USA* **108**, 1403-1408.

Huang, P., He, Z., Ji, S., Sun, H., Xiang, D., Liu, C., Hu, Y., Wang, X. and Hui, L. (2011). Induction of functional hepatocyte-like cells from mouse fibroblasts by defined factors. *Nature* **475**, 386-389.

Inoue, Y., Inoue, J., Lambert, G., Yim, S. H. and Gonzalez, F. J. (2004). Disruption of hepatic C/EBPalpha results in impaired glucose tolerance and age-dependent hepatosteatosis. *J. Biol. Chem.* **279**, 44740-44748.

Jeliazkova, P., Jors, S., Lee, M., Zimber-Strobl, U., Ferrer, J., Schmid, R. M., Siveke, J. T. and Geisler, F. (2013). Canonical Notch2 signaling determines biliary cell fates of embryonic hepatoblasts and adult hepatocytes independent of Hes1. *Hepatology* **57**, 2469-2479.

Kopp, J. L., Dubois, C. L., Hao, E., Thorel, F., Herrera, P. L. and Sander, M. (2011). Progenitor cell domains in the developing and adult pancreas. *Cell Cycle* **10**, 1921-1927.

Mackey, S. L. and Darlington, G. J. (2004). CCAAT enhancer-binding protein alpha is required for interleukin-6 receptor alpha signaling in newborn hepatocytes. *J. Biol. Chem.* **279**, 16206-16213.

Malato, Y., Naqvi, S., Schürmann, N., Ng, R., Wang, B., Zape, J., Kay, M. A., Grimm, D. and Willenbring, H. (2011). Fate tracing of mature hepatocytes in mouse liver homeostasis and regeneration. *J. Clin. Invest.* **121**, 4850-4860.

Michalopoulos, G. K. (2007). Liver regeneration. *J. Cell. Physiol.* **213**, 286-300.

Michalopoulos, G. K. (2011). Liver regeneration: alternative epithelial pathways. *Int. J. Biochem. Cell Biol.* **43**, 173-179.

Nishikawa, Y., Doi, Y., Watanabe, H., Tokairin, T., Omori, Y., Su, M., Yoshioka, T. and Enomoto, K. (2005). Transdifferentiation of mature rat hepatocytes into bile duct-like cells in vitro. *Am. J. Pathol.* **166**, 1077-1088.

Oertel, M., Rosencrantz, R., Chen, Y. Q., Thota, P. N., Sandhu, J. S., Dabeva, M. D., Pacchia, A. L., Adelson, M. E., Dougherty, J. P. and Shafritz, D. A. (2003). Repopulation of rat liver by fetal hepatoblasts and adult hepatocytes transduced ex vivo with lentiviral vectors. *Hepatology* **37**, 994-1005.

Parviz, F., Matullo, C., Garrison, W. D., Savatski, L., Adamson, J. W., Ning, G., Kaestner, K. H., Rossi, J. M., Zaret, K. S. and Duncan, S. A. (2003). Hepatocyte nuclear factor 4alpha controls the development of a hepatic epithelium and liver morphogenesis. *Nat. Genet.* **34**, 292-296.

Sasaki, K., Kon, J., Mizuguchi, T., Chen, Q., Ooe, H., Oshima, H., Hirata, K. and Mitaka, T. (2008). Proliferation of hepatocyte progenitor cells isolated from adult human livers in serum-free medium. *Cell Transplant.* **17**, 1221-1230.

Sastre, M., Steiner, H., Fuchs, K., Capell, A., Multhaup, G., Condron, M. M., Teplow, D. B. and Haass, C. (2001). Presenilin-dependent gamma-secretase processing of beta-amyloid precursor protein at a site corresponding to the S3 cleavage of Notch. *EMBO Rep.* **2**, 835-841.

Sekine, K., Chen, Y. R., Kojima, N., Ogata, K., Fukamizu, A. and Miyajima, A. (2007). Foxo1 links insulin signaling to C/EBPalpha and regulates gluconeogenesis during liver development. *EMBO J.* **26**, 3067-3615.

Sekiya, S. and Suzuki, A. (2011). Direct conversion of mouse fibroblasts to hepatocyte-like cells by defined factors. *Nature* **475**, 390-393.

Sekiya, T., Muthurajan, U. M., Luger, K., Tulin, A. V. and Zaret, K. S. (2009). Nucleosome-binding affinity as a primary determinant of the nuclear mobility of the pioneer transcription factor FoxA. *Genes Dev.* **23**, 804-809.

Senga, K., Mostov, K. E., Mitaka, T., Miyajima, A. and Tanimizu, N. (2012). Grainyhead-like 2 regulates epithelial morphogenesis by establishing functional tight junctions through the organization of a molecular network among claudin3, claudin4, and Rab25. *Mol. Biol. Cell* **23**, 2845-2855.

Si-Tayeb, K., Noto, F. K., Nagaoka, M., Li, J., Battle, M. A., Duris, C., North, P. E., Dalton, S. and Duncan, S. A. (2010). Highly efficient generation of human hepatocyte-like cells from induced pluripotent stem cells. *Hepatology* **51**, 297-305.

Tanimizu, N. and Miyajima, A. (2004). Notch signaling controls hepatoblast differentiation by altering the expression of liver-enriched transcription factors. *J. Cell Sci.* **117**, 3165-3174.

Tanimizu, N., Nishikawa, M., Saito, H., Tsujimura, T. and Miyajima, A. (2003). Isolation of hepatoblasts based on the expression of Dlk/Pref-1. *J. Cell Sci.* **116**, 1775-1786.

Tanimizu, N., Miyajima, A. and Mostov, K. E. (2007). Liver progenitor cells develop cholangiocyte-type epithelial polarity in three-dimensional culture. *Mol. Biol. Cell* **18**, 1472-1479.

Yamanaka, S. and Blau, H. M. (2010). Nuclear reprogramming to a pluripotent state by three approaches. *Nature* **465**, 704-712.

Yamasaki, H., Sada, A., Iwata, T., Niwa, T., Tomizawa, M., Xanthopoulos, K. G., Koike, T. and Shiojiri, N. (2006). Suppression of C/EBPalpha expression in periportal hepatoblasts may stimulate biliary cell differentiation through increased Hnf6 and Hnf1b expression. *Development* **133**, 4233-4243.

Yang, L. (2011). From fibroblast cells to cardiomyocytes: direct lineage reprogramming. *Stem Cell Res. Ther.* **2**, 1.

Zong, Y., Panikkar, A., Xu, J., Antoniou, A., Raynaud, P., Lemaigre, F. and Stanger, B. Z. (2009). Notch signaling controls liver development by regulating biliary differentiation. *Development* **136**, 1727-1739.

HEPATOLOGY
Official Journal of the American Association for the Study of Liver Diseases

Differentiation Capacity of Hepatic Stem/Progenitor Cells Isolated From D-Galactosamine-Treated Rat Livers

Norihisa Ichinohe,[1] Naoki Tanimizu,[1] Hidekazu Ooe,[1] Yukio Nakamura,[1,2] Toru Mizuguchi,[2] Junko Kon,[1] Koichi Hirata,[2] and Toshihiro Mitaka[1]

Oval cells and small hepatocytes (SHs) are known to be hepatic stem and progenitor cells. Although oval cells are believed to differentiate into mature hepatocytes (MHs) through SHs, the details of their differentiation process are not well understood. Furthermore, it is not certain whether the induced cells possess fully mature functions as MHs. In the present experiment, we used Thy1 and CD44 to isolate oval and progenitor cells, respectively, from D-galactosamine-treated rat livers. Epidermal growth factor, basic fibroblast growth factor, or hepatocyte growth factor could trigger the hepatocytic differentiation of sorted Thy1$^+$ cells to form epithelial cell colonies, and the combination of the factors stimulated the emergence and expansion of the colonies. Cells in the Thy1$^+$-derived colonies grew more slowly than those in the CD44$^+$-derived ones *in vitro* and *in vivo* and the degree of their hepatocytic differentiation increased with CD44 expression. Although the induced hepatocytes derived from Thy1$^+$ and CD44$^+$ cells showed similar morphology to MHs and formed organoids from the colonies similar to those from SHs, many hepatic differentiated functions of the induced hepatocytes were less well performed than those of mature SHs derived from the healthy liver. The gene expression of cytochrome P450 1A2, tryptophan 2,3-dioxygenase, and carbamoylphosphate synthetase I was lower in the induced hepatocytes than in mature SHs. In addition, the protein expression of CCAAT/enhancer-binding protein alpha and bile canalicular formation could not reach the levels of production of mature SHs. *Conclusion*: The results suggest that, although Thy1$^+$ and CD44$^+$ cells are able to differentiate into hepatocytes, the degree of maturation of the induced hepatocytes may not be equal to that of healthy resident hepatocytes. (HEPATOLOGY 2012; 57:1192-1202)

The liver normally exhibits a very low level of cell turnover, but when loss of mature hepatocytes (MHs) occurs, a rapid regenerative response is elicited from all cell types in the liver to restore the organ to its initial state. The loss may occur as a result of toxic injury, viral infection, trauma, or surgical resection. Because hepatocytes are the major functional cells of the liver, large-scale hepatocytic loss becomes a trigger for regeneration, and replication of existing hepatocytes is generally the quickest, most efficient way to compensate for the lost functions. However, when the replication of hepatocytes is delayed or entirely inhibited, hepatic stem/progenitor cells (HPCs) are activated.[1-3] As HPCs, oval cells and small hepatocytes (SHs) are well known. Oval cells were first reported to be cells that possessed an ovoid nucleus and

Abbreviations: Abs, antibodies; AFP, alpha-fetoprotein; Alb, albumin; BC, bile canaliculus; bFGF, basic fibroblast growth factor; BrdU, 5-bromo-2'-deoxyuridine; BW, body weight; CPS-I, carbamoylphosphate synthetase I; CK, cytokeratin; C/EBP, CCAAT/enhancer-binding protein; CYP1A2, cytochrome P450 1A2; 3D, three-dimensional; DPPIV, dipeptidylpeptidase IV; ECM, extracellular matrix; EGF, epidermal growth factor; FD, fluorescent diacetate; FGF, fibroblast growth factor; GalN, D-galactosamine; HA, hyaluronic acid; HGF, hepatocyte growth factor; HNF, hepatocyte nuclear factor; HPCs, hepatic stem/progenitor cells; ICC, immunocytochemistry; INF-γ, interferon-gamma; IP, intraperitoneally; LI, labeling index; MH, mature hepatocyte; mRNA, messenger RNA; PBS, phosphate-buffered saline; PH, partial hepatectomy; qPCR, quantitative polymerase chain reaction; RET, retrorsine; SH, small hepatocyte; TAT, tyrosine aminotransferase; TGF, transforming growth factor; TNF-α, tumor necrosis factor alpha; TDO, tryptophan 2,3-dioxygenase;

From the [1]Department of Tissue Development and Regeneration, the Research Institute for Frontier Medicine, and [2]First Department of Surgery, Sapporo Medical University School of Medicine, Sapporo, Japan.

Received January 31, 2012; accepted September 8, 2012.

This work was supported by the Ministry of Education, Culture, Sports, Science, and Technology, Japan, Grant-in-Aid for Scientific Research (C) (19566021; to N.I.), Grants-in-Aid for Young Scientists (B) (22790385, to N.I.; and 19790294, to J.K.), a grant from the Yuasa Memorial Foundation (to T.M.), and Grants-in-Aid for Scientific Research (B) (22390259, to K.H.; and 21390365, to T.M.), a program for developing the supporting system for upgrading the education and research (to T.M.).

Dr. Kon is currently affiliated with Gene Techno Science Co. Ltd., Sapporo, Japan.

scant cytoplasm.[4] The appearance of oval cells has been reported in rat livers treated with hepatotoxins, such as 2-acetylaminofluorene (2-AAF), combined with partial hepatectomy (PH) and D-galactosamine (GalN).[1,5–7] In GalN-induced rat liver injury, it has been shown that oval cells appear in the periportal area and differentiate into MHs through basophilic small-sized ones.[8,9] Oval cells show a wide range of phenotypic heterogeneity, and cytokeratins (CKs) 7 and 19, alpha-fetoprotein (AFP), CD34, c-kit, and Thy1 have been reported as markers for them.[1,2,5–7]

On the other hand, SHs are a subpopulation of hepatocytes, and cells isolated from healthy adult rats[10,11] and human livers[12] can clonally proliferate to form colonies and differentiate into MHs *in vitro*.[11,13] Recently, we identified CD44 as a specific marker of SHs.[14] In GalN-treated rat livers, $CD44^+$ cells appear near the periportal area between $Thy1^+$ oval cells and resident hepatocytes soon after the emergence of $Thy1^+$ oval cells.[15] In addition, we previously showed that $Thy1^+$ oval cells differentiate into hepatocytes through $CD44^+$ cells.[15,16] Our data suggested that cells sequentially converted from $Thy1^+CD44^-$ to $Thy1^+CD44^+$ and then to $Thy1^-CD44^+$ cells during the process of hepatocytic differentiation of oval cells.[15,16] Furthermore, sorted $Thy1^+$ and $CD44^+$ cells could repopulate host livers when they were transplanted into rat livers treated with retrorsine (RET) and two-thirds PH.

Although most oval cells are thought to differentiate into MHs, the details of their differentiation process, such as factors for hepatic commitment, characteristics of intermediate cells, and their fates are not well understood. In addition, it has not been elucidated whether the induced hepatocytes differentiate to possess the same capabilities as MHs. In the present experiment, we aimed to clarify which factors might induce hepatocytic differentiation of $Thy1^+$ cells and to examine how $Thy1^+$ cells could differentiate into hepatocytes through $CD44^+$ cells. In addition, we examined whether the $Thy1^+$ and $CD44^+$ cells could differentiate into fully MHs, as with those in the healthy adult liver.

Materials and Methods

Animals and Liver Injury Model. Male F344 rats (dipeptidylpeptidase IV $[DPPIV]^+$ strain; Sankyo Lab Service Corporation, Inc., Tokyo, Japan), weighing 150-200 g, were used. All animals received humane care, and the experimental protocol was approved by the committee on laboratory animals according to Sapporo Medical University guidelines. For GalN-injured livers, GalN (75 mg/100 g body weight [BW] dissolved in phosphate-buffered saline [PBS]; Acros, Geel, Belgium) was intraperitoneally (IP) administered.[14] For the transplantation experiment, female F344 rats ($DPPIV^-$ strain; Charles River Laboratories, Wilmington, MA) were (IP) given two injections of RET (30 mg/kg BW; Sigma-Aldrich Chemical Co., St. Louis, MO), 2 weeks apart,[17] and 4 weeks after the second injection, two-thirds PH was performed (RET/PH liver). Sorted $DPPIV^+$ cells (5×10^5 cells/0.5 mL) were transplanted into RET/PH livers ($DPPIV^-$) through the spleen (at least 3 rats per group).

Isolation and Culture of Cells. Rats were used to isolate hepatic cells by the collagenase perfusion method, as previously described.[18] After perfusion, the cell suspension was centrifuged at $50 \times g$ for 1 minute. The supernatant and the precipitate were used for sorting $Thy1^+$ and $CD44^+$ cells and preparing MHs, respectively. The procedure used for cell sorting was as previously described,[15] with some modifications. Antibodies (Abs) used for cell sorting are listed in Supporting Table 1. $Thy1^+CD44^+$ cells were sorted from $CD44^+$ cell and $Thy1^+$ cell fractions by using anti-Thy1 or CD44 Abs, respectively, and both were pooled. Furthermore, $Thy1^+$ and $CD44^+$ cells were also separated from $CD44^-$ and $Thy1^-$ cell fractions, respectively. After the number of viable cells was counted, 1×10^5 viable cells were plated in 12-well plates (Corning Inc., Corning, NY) and cultured in the medium listed in Supporting Table 2. The medium was replaced with fresh medium thrice-weekly.

To examine whether cells in the colonies could fully differentiate into MHs and form functional bile canaliculi (BCs), $Thy1^+CD44^-$ and $Thy1^-CD44^+$ cells sorted from GalN-D3 and SHs derived from a healthy liver were cultured for 10 days. Thereafter, some dishes were treated with Matrigel (BD Biosciences, San Diego, CA) for 10 days. To enhance the organoid formation of the colonies, as previously reported,[19]

Address reprint requests to: Norihisa Ichinohe, D.D.S., Ph.D., Department of Tissue Development and Regeneration, Research Institute for Frontier Medicine, Sapporo Medical University School of Medicine, South-1, West-17, Chuo-ku, Sapporo 060-8556, Japan. E-mail: nichi@sapmed.ac.jp; fax: +81-11-615-3099.

View this article online at wileyonlinelibrary.com.
DOI 10.1002/hep.26084
Potential conflict of interest: Nothing to report.
Additional Supporting Information may be found in the online version of this article.

colonies were separated from dishes by using Cell Dissociation Solution (Sigma-Aldrich), and colonies (2×10^3) were replated on collagen-coated dishes. Cells were cultured in the induction medium (Supporting Table 2) for 14 days. Cloning rings were used to isolate total RNA of each colony. At least two separate experiments were performed, and more than five colonies were investigated.

GeneChip Analysis, RNA Isolation, and Real-Time Polymerase Chain Reaction. Details are shown in the Supplementary Methods.

Immunostaining. For detecting $CD44^+$ colonies, cells were fixed with cold absolute ethanol at 10 days after plating, and immunocytochemistry (ICC) for CD44 was carried out. Details of staining were previously reported.[15] The numbers of $CD44^+$ colonies at days 5 and 10 were counted, and positivity was calculated. Three separate experiments were performed. To measure the labeling index (LI), 40 μM of 5-bromo-2'-deoxyuridine (BrdU) were added to the medium 24 hours before fixation. In double ICC for CD44 and BrdU, a combination of the avidin-biotin peroxidase complex method (Vectastain ABC Elite Kit; Vector Laboratories Inc., Burlingame, CA) and the alkaline phosphatase method was used. For fluorescent immunohistochemistry, sliced liver samples were frozen using isopentane/liquid nitrogen, and materials were kept at −80°C until use. All Abs used for immunostaining are listed in Supporting Table 1. Sections were embedded with 90% glycerol including 0.01% *p*-phenylenediamine and 4,6-diamidino-2-phenylindole. A confocal laser microscope (Olympus, Tokyo, Japan) was used for observation, and findings were analyzed using DP Manager (Olympus).

Treatment With Fluorescein Diacetate. As previously reported,[20] fluorescein diacetate (FD; Sigma-Aldrich) was dissolved in dimethyl sulfoxide, and the solution was diluted with the culture medium. Then, 0.25% FD was added to the medium, and the dish was rinsed three times with warm PBS. Fluorescent images were immediately photographed using a phase-contrast microscope equipped with a fluorescence device (Olympus).

Enzyme Histochemisty for DPPIV. To identify donor cells, enzyme histochemistry for DPPIV was carried out. DPPIV enzyme activity was detected as previously described.[15] $DPPIV^+$ foci in livers were photographed using a microscope equipped with a CCD camera, and the area of each focus was measured using ImageJ software (http://rsb.info.nih.gov/ij/index.html).

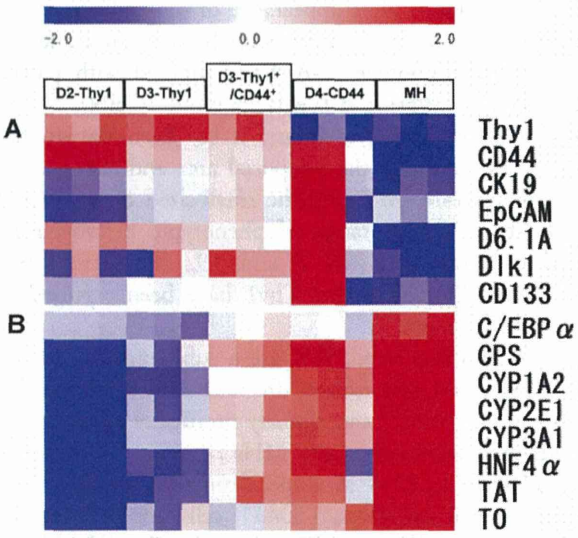

Fig. 1. Gene expression of sorted GalN-D2-$Thy1^+$ cells, D3-$Thy1^+$ cells, D3- $Thy1^+/CD44^+$ cells, and D4-$CD44^+$ cells. The gene-expression pattern of sorted cells was analyzed using GeneChip (Affymetrix, Inc., Santa Clara, CA). MHs isolated from a healthy adult rat liver were used as a control. A heatmap for genes that are classified into (A) stem cell and HPC markers and (B) hepatic markers. Relative expression of genes is shown in $\log_2$ scale. Increases in mRNA level are represented as shades of red and decreases as shades of blue.

Statistical Analysis. All data were analyzed using Turkey-Kramer's multiple comparison test. Level of statistical significance was $P < 0.05$. Experimental results are expressed as the geometric mean ± standard deviation.

Results

Characterization of Isolated Cells From Livers Treated by GalN. As previously reported,[15] $Thy1^+$ cells differentiated into hepatocytes through a $CD44^+$ intermediate state, as shown with clonally cultured $Thy1^+$ cells and cell transplantation. This transition likely happened in the GalN-treated rat liver as well. GeneChip data (Affymetrix, Inc., Santa Clara, CA) indicated that the immature hepatocyte markers, Dlk[21] and AFP were up-regulated in $Thy1^+CD44^+$ and $Thy1^-CD44^+$ cells, whereas markers related to hepatic differentiation were gradually up-regulated during the transition from Thy1-D2 to CD44-D4 cells (Fig. 1). The results also suggested that most D2-$Thy1^+$ cells were not committed to the hepatic lineage. This is consistent with our previous finding that $Thy1^+$ cells isolated from GalN-D2 could form a few epithelial cell colonies in the standard medium for SH induction, whereas those from GalN-D3 certainly formed colonies consisting of $CD44^+$ cells. Therefore, we

Table 1. Effects of Growth Factors and Cytokines on the Formation of Epithelial Cell Colonies

Growth Factors	Numbers of Colonies/Well	Numbers of Cells/Colony
Control	0	0
EGF	4.5 ± 3.8	41.4 ± 1.8
bFGF	0.3 ± 0.6	13.0 ± 0.0
HGF	1.0 ± 1.7	24.6 ± 11.7
LIF	0	0
TNF-α	0	0
IFN-γ	0	0
OSM	0	0
PDGF-BB	0	0
SCF	0	0
IL-6	0	0
TGF-β1	0	0
TGF-β2	0	0

Abbreviations: LIF, leukemia inhibitory factor; OSM, oncostatin M; PDGF-BB, plate-let-derived growth factor BB; SCF, stem cell factor.

considered the possibility that Thy1$^+$ cells became the hepatocyte lineage between D2 and D3. To specify the factors that trigger hepatic commitment, we compared expression patterns of genes related to receptors of growth factors and cytokines and selected 12 candidates (Table 1).

Induction of Epithelial Cell Colonies by Growth Factors. D2-Thy1$^+$ cells were cultured in the medium supplemented with each factor. To elucidate the formation of epithelial cell colonies, ICC for CD44 was conducted 10 days after plating. Of the 12 candidates, only epidermal growth factor (EGF), basic fibroblast growth factor (bFGF), and hepatocyte growth factor (HGF) could induce colonies (Fig. 2A; Table 1). CD44 expression of cells varied among the colonies, and some colonies consisted of cells with low expression of CD44 (CD44$^-$ cells). Next, we examined whether bFGF and/or HGF could enhance the formation and expansion of colonies in the culture with EGF (Fig. 2B). Compared to EGF only (control), the addition of bFGF or HGF did not enhance the frequency of colony formation. In the combination of EGF and bFGF or HGF, the number of cells per colony increased to twice as many as in the control (Fig. 2C). In addition, the combination of the three factors also dose dependently increased the number of cells per colony. These results suggested that a certain number of Thy1$^+$ cells possessed the ability to differentiate into hepatic cells, and that the induction was initiated by EGF, bFGF, and/or HGF.

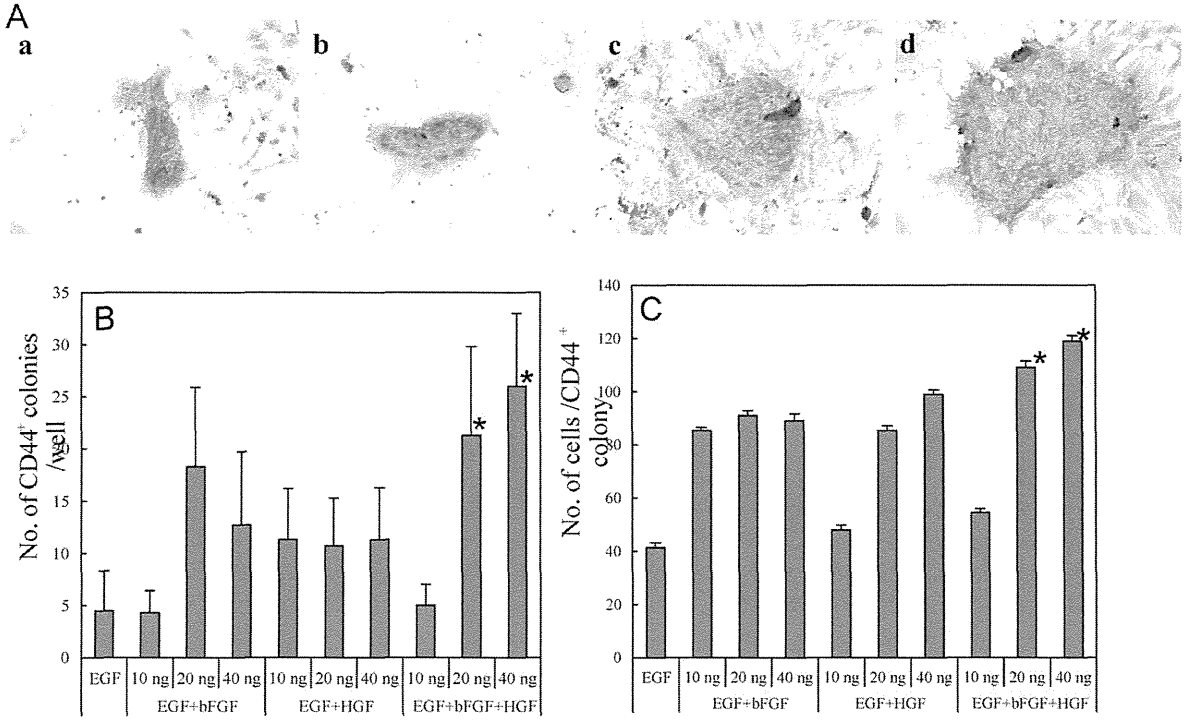

Fig. 2. Induction of CD44-positive cell colonies from sorted D2-Thy1$^+$ cells by treatment with EGF, bFGF, and/or HGF. Thy1$^+$ cells (1×10^5 viable cells/well) sorted from the GalN-D2 liver were plated on 12-well plates and cultured in medium supplemented with EGF (a), EGF+bFGF (b), EGF+HGF (c), and EGF+bFGF+HGF (d) for 10 days. Dose dependency of colony formation was examined. To identify colonies, ICC for CD44 was carried out. The number of CD44$^+$ cell colonies per well (B) and that of cells per colony (C) were measured. Asterisks shown in (B) and (C) indicate significance: $P < 0.05$, compared to EGF and 10 ng of EGF+bFGF+HGF.

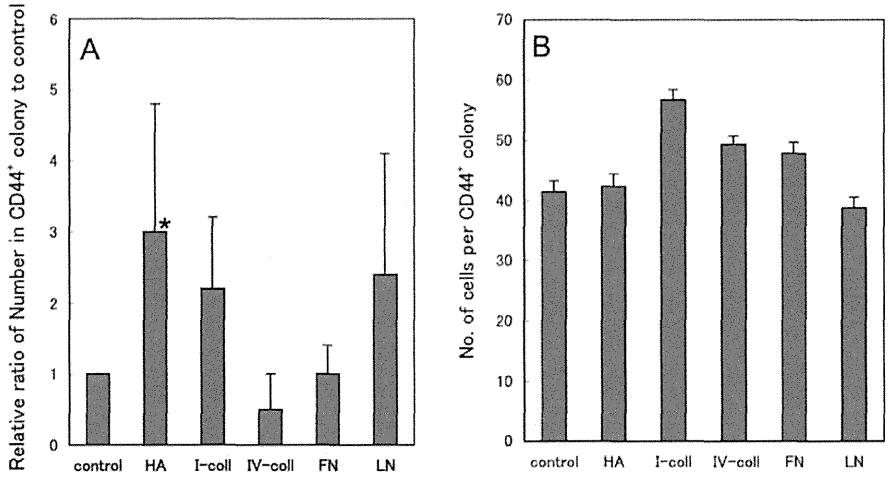

Fig. 3. Effects of ECM on colony formation of Thy1$^+$ cells were investigated. Thy1$^+$ cells were isolated from GalN-D2 rat livers and plated on dishes coated with hyaluronic acid (HA), type I collagen (I-coll), type IV collagen (IV-coll), fibronectin (FN), and laminin (LN). Noncoated dishes were used as controls. Cells were cultured in medium with EGF. To identify the colony, ICC for CD44 was carried out. The number of CD44$^+$ cell colonies per dish (A) and that of cells per colony (B) were measured. Asterisk shows significance: $P < 0.05$, control versus HA.

Induction of Epithelial Cell Colonies by Extracellular Matrix. Because CD44 is one of the receptors of hyaluronic acid (HA)[22,23] and because SHs can selectively proliferate on HA,[18] we investigated whether extracellular matrix (ECM) affected the frequency of emergence and phenotype of colonies derived from D2-Thy1$^+$ cells. Sorted D2-Thy1$^+$ cells were cultured on dishes coated with type I collagen, fibronectin, laminin, and HA, and ICC for CD44 was performed 10 days after plating. When cells were cultured in the medium supplemented with EGF, frequency of colony formation was significantly higher for cells on HA-coated dishes than for the control (Fig. 3A), but no difference was observed in the number of cells per colony among the dishes with each ECM (Fig. 3B).

Growth Ability and CD44 Expression of Cells Sorted From GalN-D3. Thy1$^+$CD44$^-$ (Thy1), Thy1$^+$CD44$^+$, and Thy1$^-$CD44$^+$ (CD44) cells sorted from a GalN-D3 liver were cultured in the medium with EGF for 10 days. Double ICC for CD44 and BrdU was carried out (Fig. 4A–C). The frequency of colony formation was more than four times higher for CD44 cells than for both Thy1 and Thy1$^+$CD44$^+$ cells (Fig. 4D), and the average number of cells per colony was significantly larger for CD44 cells than for Thy1 and Thy1$^+$CD44$^+$ cells (Fig. 4E). The percentages of BrdU$^+$ cells were approximately 70% and 80% in colonies derived from Thy1 and CD44 cells, respectively (Fig. 4A–C, F). Growth ability of Thy1$^+$CD44$^+$ cells was also intermediate between those of Thy1 and CD44 cells.

Intensity and the localization of CD44 varied among cells forming colonies. In spite of the origin of sorted cells, CD44 protein was usually expressed in cell membranes between cells (Fig. 4C). Some colonies consisted of cells with CD44 protein localized in both the cell membrane and cytoplasm (Fig. 4A, B). The latter type of colony was often observed in the culture of Thy1 cells. CD44 positivity of Thy1$^+$ cells in a colony was approximately 65% at day 5 and increased to approximately 80% at day 10 (Fig. 4G).

Next, to examine whether acquisition of CD44 expression in Thy1$^+$ cells was also correlated to growth ability of cells *in vivo*, cell transplantation was carried out. D2-Thy1$^+$, D3-Thy1$^+$CD44$^-$, D3-Thy1$^+$CD44$^+$, D3-Thy1$^-$CD44$^+$, and D4-CD44$^+$ cells (5×10^5 cells/rat) isolated from GalN-treated livers were intrasplenically transplanted into RET/PH-treated rats. One month after transplantation, the number of cells in foci derived from D4-CD44 was much larger than in those from Thy1-expressing cells (Fig. 4H, I). The growth rate of engrafted cells increased in correlation with the expression of CD44 and time after GalN treatment. In addition, no types of donor-derived (Y chromosome$^+$) cells, other than hepatocytes, could be found in recipient livers (Supporting Fig. 1).

Gene Expression of Hepatic Markers of Epithelial Cell Colonies Derived From D3-Thy1 Cells. To elucidate the characteristics of cells in colonies derived from D3-Thy1 cells, quantitative polymerase chain reaction (qPCR) of cells was performed for each colony, which was separated from the culture dish using a